

SURVEY PAPER

THE DERIVATION OF THE GENERALIZED FUNCTIONAL EQUATIONS DESCRIBING SELF-SIMILAR PROCESSES

Raoul R. Nigmatullin ¹, Dumitru Baleanu ^{2,3}

Abstract

The generalized functional equations describing a wide class of different self-similar processes are derived. These equations follow from the observation that microscopic function describing an initial self-similar process increases monotonically or even cannot have a certain value. The last case implies the behavior of trigonometric functions $\cos(z\xi^n)$, $\sin(z\xi^n)$ at $\xi > 1$ and n >> 1 that can enter to the microscopic function and when the limits of the initial scaling region are increasing and becoming large. The idea to obtain the desired functional equations is based on the approximate decoupling procedure reducing the increasing microscopic function to the linear combination of the same microscopic functions but having smaller scales. Based on this idea the new solutions for the well-known Weierstrass-Mandelbrot function were obtained. The generalized functional equations derived in this paper will help to increase the limits of applicability in description of a wide class of self-similar processes that exist in nature. The procedure that is presented in this paper allows to understand deeper the relationship between the procedure of the averaging of the smoothed functions on discrete self-similar structures and continuous fractional integrals.

MSC 2010: Primary 28A80; Secondary 26A33

Key Words and Phrases: self-similar (fractal) processes; Weierstrass-Mandelbrot function; fractional calculus; solutions of functional equations

^{© 2012} Diogenes Co., Sofia

1. Introduction and formulation of the problem

With the appearance of the book B. Mandelbrot [6] many researches are trying to apply the ideas of fractal geometry and self-similarity principles for description and generalization of different phenomena and processes that exist in nature. In order to obtain the desired power-law exponents many authors simply replace the integer values of derivatives/integrals by similar non-integer differentiation/integration operators in many basic equations of physics, including diffusion, wave and other equations. Many examples of replacements of such kind can be found in books [15, 2, 17], also paper [4] and references therein, reflecting the modern state of the interdisciplinary direction having acronym "FDA" (Fractional Derivative and its Applications). Despite of the essential progress that was achieved by many researches actively working in the field of the Fractional Calculus (FC)applications, many authors leave aside the questions of validity and justification of this replacement and the natural reasons of appearance of the non-integer differential/integral operators in basic equations that pretend on the description of dynamical processes taking place in fractal media. So, the basic question is remained and can be formulated as follows: What kind of equations (differential, integral, matrix and others) initially not having the power-law exponents have solutions containing the desired power-law functions with real or even complex-conjugated exponents? A similar question can be formulated in another form: Is there any relationship between self-similar (scaling) properties of the fractal medium (considered on the mesoscale region) with non-integer derivative/integral or not? The clear and well-justified answers for these questions are important for further applications of the apparatus of the fractional calculus in physics and other natural sciences. The basic motivation of this paper is to show how to obtain the general solutions containing a linear combination of the power-law exponents (including real and complex-conjugated values) that follow from a certain class of the functional equations. These generalized functional equations can describe a wide class of processes having a fractal nature.

The results of this survey will serve as a guideline in understanding of the relationship between non-integer operators and self-similar processes. The content of the paper is organized as follows. In Section $\mathbf 2$ we consider the model of self-similar process that includes the simplest case considered earlier in [7, 8]. The approximate analytical solutions found in Section $\mathbf 2$ are verified numerically in Section $\mathbf 3$ by application to the well-known Weierstrass-Mandelbrot (WM)-function. The results obtained in Section $\mathbf 2$ allow us to find new solutions for the WM-function that were not known before. The results and some further generalizations are summarized in the

last Section 4. We include as illustration several fugures, and two Appendices (Sections 5,6) that gives some mathematical details.

2. The model of the self-similar process

In order to understand better the new results we should remind the previous result that has been obtained in [7, 8] by one of the authors (RRN). Let us suppose that we consider a process that can be described by some variable z. This variable can accept real or even complex value (in the last case it can coincide with the argument associated with the Laplace or Fourier transformations). If in the result of the scaling transformation $z \to z\xi$ this process is not changed, then one can write the following functional equation

$$S(z\xi) = \frac{1}{b}S(z) + c_0. \tag{2.1}$$

Here z defines a current variable that can be real or complex, the real/complex values ξ , b and c_0 define the parameters of this simplest functional equation. The general solution of this functional equation was obtained in [7, 8] and can be written as

$$S(z) = PR_{\nu}(\ln z)z^{\nu} + \frac{c_0}{(1 - \frac{1}{b})}, \quad \nu = \frac{\ln(\frac{1}{b})}{\ln(\xi)},$$

$$PR_{\nu}(\ln z) = A_0 + \sum_{1}^{\infty} Ac_k \cos(2\pi k \frac{\ln z}{\ln \xi}) + As_k \sin(2\pi k \frac{\ln z}{\ln \xi}),$$

$$PR_{\nu}(\ln(z) \pm \ln(\xi)) = PR_{\nu} \ln(z). \tag{2.2}$$

The second and the third rows in (2.2) determine a unknown log-periodic function having the real period coinciding with the value $ln(\xi)$. Let us consider the sum of the type

$$S_N(z) = \sum_{n=-N+1}^{N-1} b^n f(z\xi^n).$$
 (2.3)

It appears in the result of averaging of some physical value (described by the microscopic function f(z)) over discrete fractal structure (when the volume $V_n = c_0 b^n$). The value N in (2.3) determines the limits of a selfsimilar region. This sum for any finite N has the following scaling property

$$S_N(z\xi) = \frac{1}{b}S_N(z) + b^{N-1}f(z\xi^N) - b^{-N}f(z\xi^{-N+1}).$$
 (2.4)

If the function f(z) is chosen in a way that the contribution of the last two terms in the limit $N \to \infty$ becomes negligible, then we obtain the scaling equation (2.1) with general solution (2.2). The description of some self-similar process in the form of additive combination of microscopic processes distributed over a fractal structure or in the form of the strongly-correlated

product (considered in [7, 8]) was turned to be very constructive. Later, based on this idea one of us enabled to find the physical meaning of the temporal fractional integral [8] with real and complex-conjugated power-law exponents and develop the theory of dielectric relaxation in the mesoscale region based on the fractional kinetics [9, 10] including its experimental confirmation [11, 12]. It is interesting to note also that the solution of the functional equation (2.1) at $c_0 = 0$ given in the book [3] is not complete. As it was shown in [7, 8], the log-periodic function (defined by relationship (2.2)) is reduced to the constant A_0 when the averaging procedure over the period $ln(\alpha)$ is introduced. In other words, the values ξ should be distributed over the continuous set of scales. When the distribution of the values $\xi_n(n=1,2...)$ is discrete, then the log-periodic function appearers. The French scientist D. Sornette was the first who noticed this peculiarity and now the log-periodic oscillations were discovered in many real physical processes. More details are given in his paper [16]. In our paper [13] the linear principle for the strongly-correlated variables has been formulated in order to modify the simplest functional equation (2.2) and to find new regions of its application. But in this paper the modified functional equations were written on the intuitive level without their proper derivation. The basic aim of this paper is to generalize the simplest functional equation (2.2) and to increase the limits of its applicability for a wide class of different self-similar processes that can take place in the mesoscale region.

We choose the following model of some general self-similar process. Let us suppose that this process on the subatomic level is described by some microscopic function f(z). For this concrete case the current variable z can be associated with temporal variable and corresponds to the $z=\frac{t}{\tau_c}$, where τ_c determines a characteristic time of the dynamic/relaxation process considered. The geometrical and dynamical properties associated with some self-similar region are characterized by the parameters b and ξ , correspondingly. From the mathematical point of view, the total process covering all self-similar regions can be expressed as

$$S(z) = c_0 \sum_{n = -N_0}^{N} b^n f(z\xi^n).$$
(2.5)

In contrast with the previous case (2.3), we consider more general expression. Here c_0 determines the value of the geometric variable at n=0, the values N_0 and N determine the limits of the mesoscale corresponding to the whole self-similar process. We suppose that the low limiting value $N_0(N_0 < N, N >> 1)$ corresponds to the beginning of some self-similar process both in space and time. The geometrical parameter b can be positive or even negative. Before it was supposed that microscopic function f(z) had the finite limits at small and large values of the variable z. For

this case the contribution of two terms in (2.3) is negligible and we come to solution (2.2) considered earlier. In this paper we want to consider the case when the contribution of two terms in (2.3) is essential. It means that in the limit N >> 1 the values of the function f(z) at z >> 1 become large or does not exist. The last case implicates the behavior of trigonometric functions $cos(z\xi^N)$, $sin(z\xi^N)$ at N >> 1 that can enter to the microscopic function f(z) as factors or argument. So, mathematically the behavior of f(z) can be written as

$$\lim_{N \to \infty} f(z\xi^N) = \{ \begin{array}{c} \text{does not exist,} \\ \infty, \ \xi > 1 \end{array}$$
 (2.6)

For the first case one can imply the combination of trigonometric functions (for example, the Mandelbrot-Weierstrass function). The second case can be associated with any microscopic function that is unbounded at $z\gg 1$. So, we want to find the general form of the functional equation for the Case-1: $(b,\xi>1)$. The Case-2: $(b,\xi<1)$ can be considered in complete analogy with the Case-1, making the simple replacement $b\to b^{-1}, \xi\to \xi^{-1}$. Other two possible cases determined as Case-3: with $(b>1,\xi<1)$, and Case-4: $(b<1,\xi>1)$ lead to the simple functional equation (2.1) with solution (2.2). These cases have been considered earlier in [7, 8]. If we replace z for $z\xi$ on the left-hand of relationship (2.5), then after some simple algebraic manipulations one can obtain the following identity

$$S(z\xi) = \frac{1}{b}S(z) + b^{N}f(z\xi^{N+1}) - b^{N_0 - 1}f(z\xi^{-N_0}).$$
 (2.7)

In contrast with condition (2.6) specifying the behavior of the microscopic function at z >> 1, we suppose that at small values of z there is a limit

$$\lim_{N_0 \to \infty} f(z\xi^{-N_0}) = \{ \begin{array}{c} 0 \\ L_1, \ \xi > 1 \end{array} . \tag{2.8}$$

From identity (2.7) replacing $z \to z \xi^{q-1}$, we obtain easily

$$S(z\xi^{q}) = \frac{1}{b}S(z\xi^{q-1}) + b^{N}f(z\xi^{N+q}) - b^{N_0-1}f(z\xi^{-N_0+q-1}), q = 1, 2, ..., k-1, k.$$
(2.9)

Taking into account condition (2.6) we cannot eliminate the large term $b^N f(z\xi^{N+q})$ from (2.9). In general, the infinite set of equations (2.9) contains two types of different variables $S(z\xi^q)$, $b^N f(z\xi^{N+q})(q=1,2,\cdots,k)$ and cannot be reduced to the system containing only one type of variable. In order to close the infinite chain of equations (2.9) relatively unknown function S(z) (or equally for the unknown microscopic function f(z)) we should make a reasonable supposition (it will be justified below numerically)

$$f(z\xi^{N+1}) \cong \sum_{q=1}^{k-1} C_q f(z\xi^{N+q}).$$
 (2.10)

Here C_q , $(q = 1, 2, \dots k - 1)$ a set of constants that approximate the function figuring on the left-hand side. These unknown constants can be found numerically with the help of the linear-least square method (LLSM). From the system of equations (2.9) we have

$$b^{N} f(z\xi^{N+q}) = S(z\xi^{q}) - \frac{1}{b}S(z\xi^{q-1}) + L_{q}, q = 1, 2, \dots k - 1, \qquad (2.11)$$

$$b^{-N_0 - 1} f(z\xi^{N_0 + q})^{1 \ll N_0 < N} \cong L_q. \tag{2.12}$$

Here we took into account the limit (2.12) describing approximately the behavior of f(z) for small values of z. For q = k we have from (2.9)

$$S(z\xi^k) = \frac{1}{b}S(z\xi^{k-1}) + b^N f(z\xi^{N+k}) - L_k.$$
 (2.13)

Taking into account the decoupling (2.10) and relationships (2.11) we have

$$b^{N} f(z\xi^{N+k}) \cong b^{N} \sum_{q=1}^{k-1} C_{q} f(z\xi^{N+q})$$

$$= \sum_{q=1}^{k-1} C_{q} [S(z\xi^{q}) - \frac{1}{b} S(z\xi^{q-1})] + \sum_{q=1}^{k-1} C_{q} L_{q}. \quad (2.14)$$

After some simple algebraic transformations of expression (2.13) and substitution into it expression (2.14), we obtain finally the closed functional equation relatively the remaining variable S(z)

$$S(z\xi^{k}) = \left(\frac{1}{b} + C_{k-1}\right)S(z\xi^{k-1}) + \sum_{q=1}^{k-2} \left(C_{q} - \frac{C_{q+1}}{b}\right)S(z\xi^{q})$$
$$- \frac{C_{1}}{b}S(z) + \sum_{q=1}^{k-1} C_{q}L_{q} - L_{k}. \tag{2.15}$$

So, for a wide class of self-similar processes when the condition (2.6) is essential we obtain more general functional equation (2.15) in comparison with the previous case (2.1), when the influence of the function f(z) for the both limits (z >> 1, z << 1) remains certain and finite (and in the previous cases considered two terms in (2.4) had negligible values). In the complete analogy with Case-1, one can consider Case-2: ($b, \xi < 1$). The algebraic manipulations for this case are similar and so the detailed consideration of this case is omitted. The limits of applicability of the functional equation (2.15) can be increased if we replace the initial variables

 $(ln(z) \to t, ln(\xi) \to T)$ and consider the similar processes that are shifted relatively each other to the past/future interval of time. For this case we have

$$S(t+kT) = a_{k-1}S(t+(k-1)T) + \sum_{q=1}^{k-2} a_q S(t+qT) + a_0 S(t) + B_k,$$

$$B_k = \sum_{q=1}^{k-1} C_q L_q - L_k.$$
(2.16)

Here the values of the constants $a_q(q=0,1,\cdots,k-1)$ coincide completely with the corresponding constants figuring in (2.15). The formal solutions of these functional equations (2.15) and (2.16) have been considered in the paper [13] (and in brief are listed in Mathematical Appendix 1 here, Sect. 5) and so it is not necessary to repeat these solutions again. But the functional equations (2.15) and (2.16) were written in [13] on an intuitive level without their accurate derivation and proper justification. In this paper we show how to derive them from the model of self-similar process formulated above together with intrinsic reasons that can produce the functional equations of the type (2.15) or (2.16). What kind of additional physical interpretation one can give for the function S(z)?

The function S(z) describes some dynamical one-dimensional (1D) self-similar process that takes place on a set of geometrical objects that are distributed randomly in the space and described by a set of geometric parameters $V_n = c_0 b^n$ $(n = -N_0, -N_0 + 1, \dots, N)$.

This value, for example, can be associated with a volume or another extensive statistical parameter. The microscopic dynamical process is described by the function f(z). The dynamical scale of the process is determined by parameter ξ . It can be associated, for example, with a set of relaxation times that obey to the scaling hypothesis. In the case when the function f(z) satisfying to condition (2.6) is predominant, the description of the averaged self-similar process associated with one dynamic fractal dimension is not sufficient. For Case-1 considered above, it is necessary to have a numerable set of fractal dimensions that are defined from equations

$$\nu_r = \frac{\ln(\lambda_r)}{\ln(\xi)}, \quad r = 1, 2, \cdots, \tag{2.17}$$

where the set of the parameters λ_r , in turn, are calculated as the roots of the polynomial

$$P(\lambda) = \lambda^{k} - \sum_{q=1}^{k-1} a_{q} \lambda^{q} - a_{0}, \ a_{k-1} = C_{k-1} + \frac{1}{b},$$

$$a_{q} = C_{q} - \frac{C_{q+1}}{b}, q = 1, 2, \dots, k-2, \ B_{k} = \sum_{q=1}^{k-1} C_{q} L_{q} - L_{k}. \ (2.18)$$

If the set of the roots (2.17) can be calculated analytically then the general solution of the functional equation (2.15) can be presented in the form of linear combination of power-law and log-periodic functions

$$S(z) = \sum_{r=1}^{k} PR_r(\ln(z)) z^{\nu_r} + \tilde{L_r}, \qquad (2.19)$$

when all roots of the polynomial $P(\lambda)$ are supposed to be different (the nondegenerate case). The set of $PR_r(ln(z))$ defines the unknown log-periodic functions and they can be presented by the infinite Fourier series

$$PR_r(\ln(z)) = A_0^{(r)} + \left[\sum_{k=1}^{\infty} Ac_k^{(r)} \cos(2\pi k \frac{\ln(z)}{\ln(\xi)}) + As_k^{(r)} \sin(2\pi k \frac{\ln(z)}{\ln(\xi)}) \right].$$
(2.20)

with period $ln(\xi)$. The decomposition coefficients of the series (2.20) should be found from initial or other conditions. When a root ν_r figuring in (2.17) accepts the negative value then (as it has been shown in [13]) it is necessary to replace the root by its modulus value and the periodic function in (2.20) should be replaced by some anti-periodic function having the following decomposition

$$PR_r^{(a)}(ln(z)) = \left[\sum_{k=1}^{\infty} Ac_k^{(r)} \cos(\pi k \frac{ln(z)}{ln(\xi)}) + As_k^{(r)} \sin(\pi k \frac{ln(z)}{ln(\xi)})\right]. \quad (2.21)$$

The constant $\tilde{L_k}$ figuring in (2.19) is determined by the free variation constant method and depends totally on the constant value B_k figuring in (2.18). If one of the roots of polynomial (2.18) ν_g is degenerated then the solution for this root can be written as

$$S_g(z) = \left[\sum_{s=1}^g PR_{s-1}(\ln(z))(\ln(z))^{s-1}\right] z^{\nu_g},\tag{2.22}$$

where the value g determines the degree of degeneracy. Here, again the unknown log-periodic functions entering into (2.22) are determined by decompositions (2.20), (2.21). If we replace the variables $(\ln(z) \to t, \ln(\xi) \to T)$ figuring in general solution (2.19) then one can obtain the solution of the functional equation (2.16). It is considered in the Mathematical Appendix 1, and not given here because it is obtained from (2.19) by simple replacement. Before to start considering some interesting example it is instructive to give the solution for the case k=2. As we will see below this case can be met frequently in possible applications. For this case we have the simplest decoupling

$$f(z\xi^{N+2}) \cong C_1 f(z\xi^{N+1}).$$
 (2.23)

The functional equation has the following structure

$$S(z\xi^{2}) = (\frac{1}{b} + C_{1})S(z\xi) - \frac{C_{1}}{b}S(z) + B_{2}.$$
 (2.24)

The desired polynomial and the constant from (2.24) are defined as
$$P(\lambda) = \lambda^2 - (\frac{1}{b} + C_1)\lambda + \frac{C_1}{b}, \ B_2 = C_1L_1 - L_2. \eqno(2.25)$$
 The corresponding roots and power-law fractal dimensions are calculated

easily and given by expressions

$$\lambda_1 = \frac{1}{b}, \ \lambda_2 = C_1, \ \nu_{1,2} = \frac{\ln(\lambda_{1,2})}{\ln(\xi)}.$$
 (2.26)

The general solution of the functional equation (2.24) for the nondegenerate case $(C_1, b \neq 1)$ is written as

$$S(z) = PR_1(\ln(z))z^{\nu_1} + PR_2(\ln(z))z^{\nu_2} + k_1, k_1 = \frac{B_2}{(1 - \frac{1}{h})(1 - C_1)}.$$
(2.27)

The general solution of the functional equation (2.24) for another case when $(C_1 = 1, b \neq 1)$ is written as

$$S(z) = PR_1(\ln(z))z^{\nu_1} + PR_0(\ln(z)) + k_1\ln(z), k_1 = \frac{B_2}{(1 - \frac{1}{b})\ln(\xi)}. \quad (2.28)$$

And, at last, we give the solution of (2.24) for the degenerate case $(C_1 = b = 1, g = 2)$:

$$S(z) = PR_1(\ln z) \cdot \ln(z) + PR_0 \ln(z) + k_2 \ln^2(z), \quad k_2 = \frac{B_2}{2\ln^2 \xi}.$$
 (2.29)

Finishing this section we should stress here that the set of fractal dimensions calculated from (2.17) is always discrete and does not coincide with the continuous set of dimensions associated with a multi-fractal structure [5].

3. Verification of decoupling for the generalized Weierstrass-Mandelbrot function

We like to test and demonstrate the effectiveness of the decoupling (2.10) using as an example the Weierstrass-Mandelbrot (WM)-function

$$W(x) = c_0 \sum_{n = -N_0}^{N_1} b^n \sin^2 \left(\theta + \frac{\xi^n \pi x}{2}\right).$$
 (3.1)

For $N_0, N_1 >> 1, \xi > 1, 1 < D < 2, b = \frac{1}{\xi^{(2-D)}} < 1$ this function coincides with the real part of the WM-function that is determined, for example, in the book [5]. It is easy to see that for this case when $(b < 1, \xi > 1)$ (defined above as Case-4) the influence of two last terms figuring in (2.7) at N_0 and $N_1 >> 1$ is negligible. For this case we have the standard scaling equation of the type (2.1) with solution (2.2),

$$W(x\xi) = \frac{W(x)}{b}, \ \nu = \frac{\ln(\frac{1}{b})}{\ln(\xi)} = 2 - D, \ C_0 = 0,$$

$$W(x) = PR_{\nu}(\ln(x))x^{\nu}, \ PR_{\nu}(\ln(x) \pm \ln(\xi)) = PR_{\nu}(\ln(x)). \ (3.2)$$

Other properties of this function (corresponding to Case-4) can be found in the corresponding references given in the book [5].

3.1. Analysis of the WM-function for $(b > 1, \xi > 1, b < \xi)$

Figures 1 (a, b, c) show the behavior of this function for N=25, 100, 1000 reference points. The concrete values of the parameters are taken as:

$$c_0 = 10^{-6}, b = 1.25, \xi = 1.5, N_0 = 10, N_1 = 60, \theta = \frac{\theta}{4}.$$
 (3.3)

Verification of the hypothesis (1.8): For the given value of $N_1 = 60$ direct numerical calculations of the function

$$f(x\xi^{N_1+k}) = \sin^2(\theta + \frac{\pi x}{2}\xi^{N_1+k}), \ k = 0, 1, \dots, K,$$
 (3.4)

lead to the following relationship:

$$f(z\xi^{N_1+k}) \cong f(z\xi^{N_1+k-1}), C_{k-1} = 1, C_q = 0, \text{ for } q = 1, 2, \dots, k.$$
 (3.5)

Figures 2 (a,b,c) clearly demonstrate the validity of relationship (3.5) for all possible values of k if the value of N_1 is sufficiently large. Number of calculated points (N = 25, 100, 1000) and the values of parameters from (3.3) used for verification of relationship (2.12) conserve their values. So, this simple test leads us to the functional equation (24) where we put $C_1 = 1, C_0 = 0$:

$$S(z\xi^2) = (1 + \frac{1}{b})S(z\xi) - \frac{1}{b}S(z) - \Delta L_1.$$
 (3.6)

The constant ΔL_1 is obtained as a difference between the arithmetic mean values of the limiting functions

$$\Delta L_1 = mean \left[b^{-N_0 - 1} \left(f(z\xi^{-N_0 + 2}) - f(z\xi^{-N_0 + 1}) \right) \right]. \tag{3.7}$$

These functions are plotted in **Figure 3**. As one can see from this figure, their deviations are really small and this observation helps us to replace them by their mean values in order to obtain the desired value ΔL_1 . The value of this constant lies in the interval [0.01, 0.03] for all range of the reference points considered and so its influence is not important for further analysis. Following to the general result expressed by relationship (2.28), we rewrite the solution (3.6) for the numerical tests as

$$S(z) = PR_0 ln(z) + PR_{\nu} ln(z) z^{\nu} + k_1 ln(z). \tag{3.8}$$

Here $\nu = ln(1/b)/ln(\xi)$ is one of the roots of the scaling equation

$$\lambda^{2} - (1 + \frac{1}{b})\lambda + \frac{1}{b} = 0, \quad \lambda_{1,2} = 1, \frac{1}{b},$$

$$\nu_{1,2} = 0, \quad \frac{\ln(\frac{1}{b})}{\ln(\xi)}.$$
(3.9)

The value of the constant k_1 figuring in (3.8) (obtained as before by the variation of a free constant method) is determined by expression

$$k_1 = \frac{-\Delta L_1}{(1 - \frac{1}{h})ln(\xi)}. (3.10)$$

The unknown periodic functions $PR_{0,\nu}(ln(z))$ from (3.8) are given by expression (2.20). The amplitudes $A_0^{(0,\nu)}, Ac_k^{(0,\nu)}, As_k^{(0,\nu)}$ can be found from the given initial conditions or from the direct fitting of the solution (3.8) to W(x) from (3.1) by the linear least square method (LLSM). We realized the numerical test of solution (3.8) for the given reference points (25, 100, 1000) using the set of constants from (32). The results of the fitting are illustrated by **Figures 4** (a,b,c). We want to stress here the following fact. With increasing of number of reference points the results of the fitting are becoming worse and number of the fitting constants (figuring in expression (2.20) in order to achieve an acceptable accuracy are increased essentially. We are not giving them because their concrete values are not important for this test analysis. Additional details related to the application of the fitting procedure are explained in the captions to Figures 4(a,b,c). Finishing this section one can say that new solution (3.8) found for the WM-function increases our understanding of some hidden features that can be found for self-similar processes covering by expression (2.5).

3.2. Analysis of the WM-function for $(b = 1, \xi > 1)$ (The degenerate case)

It is useful to write the solution of the scaling equation for the WMfunction for the degenerate case. It follows from expression (2.29)

$$S(z) = [PR_0^1(\ln(z))] \ln(z) + Pr_0^{(0)}(\ln(z)) + k_2 \ln^2(z).$$
 (3.11)

Here, again we have two unknown log-periodic functions $PR_0^{0.1}(ln(z))$ that can be decomposed to the Fourier series (2.20). The value k_2 can be found again by the variation of a free constant method and is written as

$$k_2 = -\frac{\Delta L}{2ln^2(\xi)} \,. \tag{3.12}$$

So, for this case we do not have the power-law behavior (as it might expect) and for this degenerate case the power-law exponent is reduced to the logarithmic function. For the given reference points (25, 100, 1000) the results of the fitting are illustrated by **Figures 5** (a,b,c). Other features are remained the same and so similar figures that we had for the previous case are omitted.

4. Results and new possibilities

The basic result obtained in this paper can be formulated as follows. Based on a simple (1D) model of self-similar process presented by expression (1.5) and taking into account the different behavior of the microscopic function f(z) (2.6) one can derive more general functional equation (2.15). This generalized equation contains a countable set of dimensions and so description of a self-similar process by one fractal dimension is not complete. The different asymptotic behavior of the microscopic function f(z) requires for description of a general self-similar processes the finite set of dimensions. Here we want to pay attention of a potential reader for new possibilities and possible generalizations of these results. If the self-similar process takes place in two directions then instead of equation (2.5) we have the following sum

$$S(z) = c_0 \sum_{n_1 = -N_1}^{N_1} \sum_{n_2 = -N_2}^{N_2} b_1^{n_1} b_2^{n_2} f(z \xi_1^{n_1} \xi_2^{n_2}).$$
 (4.1)

The detailed consideration of this important case (closely associated with practical applications) merits a special research because it needs to consider 6 different cases. The simplest case of the functional equation obtained for the variable S(z) has been derived and considered in paper [1] and has the form

$$S(z\xi_1\xi_2) = a_{00}S(z) + a_{10}S(z\xi_1) + a_{01}S(z\xi_2) + F_0.$$
(4.2)

The solutions of the functional equation (4.2) were applied successively for consideration of the properties of 2D self-similar (fractal) circuits containing RC-elements. The generalization of (4.1) when F_0 in (4.2) is not a constant merits a separate research. Another interesting possibility in deeper understanding of different self-similar processes is related to conception of the quasi-fractals (Q-fractals). These fractals with another type of scaling were defined on intuitive level (without their proper justification) in paper [14]. So, here we want to show how to consider the self-similar processes and derive the corresponding functional equation that can take place in structures having another type of scaling. Let us suppose that the total self-similar process that takes place in a fractal medium describing by the Q-fractals can be presented by the sum of the type

$$S(z) = c_0 \sum_{j=1}^{N} j^b f(zj^{\xi}). \tag{4.3}$$

Here the constants c_0 have the same meaning as before but the type of scaling (in comparison with the sum from (2.5)) is totally different. In expression (4.3) the value b numerates the geometrical objects while index ξ is associated with dynamic process that can take place in the region of

the mesoscale. The argument z as before can accept the real or complex values. The index j numerates the number of objects obeying this scaling hypothesis. These Q-fractals has logarithmic scaling. In order to see it we present the last sum in the equivalent form

$$S(z) = c_0 \sum_{j=1}^{N} b^{l\tilde{n}(j)} f(z\tilde{\xi}^{lnj}), \quad \tilde{b} = \exp(b), \quad \tilde{\xi} = \exp(\xi).$$
 (4.4)

If we replace formally the summation index $n=\ln(j)$, then we obtain expression similar to the sum (2.3) but with one principle difference (all index values j (j=1,2,...,N) figuring in the modified sum (4.4) should keep their integer values). In order to apply the same idea for obtaining the scaling equation for the sum (4.4) we present it in the following form

$$S(z\tilde{\xi}^a) = c_0 \sum_{j=1}^N \tilde{b}^{lnj} f(z\tilde{\xi}^{ln(jexp(a))}). \tag{4.5}$$

In the expression (4.5) a is unknown constant. If we put a = ln2, then making the replacement of initial index j for $j' = \exp(a)j = 2j$, we transform (4.5) to the following form

$$S(z\tilde{\xi}^{ln(2)}) = \frac{c_0}{\tilde{b}^{ln(2)}} \sum_{j=2}^{2N} \tilde{b}^{ln(j)} f(z\tilde{\xi}^{ln(j)}) = \frac{S(z)}{\tilde{b}^{ln(2)}} - \frac{c_0}{\tilde{b}^{ln(2)}} f(z) + R_N(z),$$

$$R_N(z) = \frac{c_0}{\tilde{b}^{ln(2)}} \sum_{j=2}^{2N} \tilde{b}^{ln(j)} f(z\tilde{\xi}^{ln(j)}). \tag{4.6}$$

The evaluation of the last sum $R_N(z)$ is given in Mathematical Appendix 2, Section 6. So, the further investigation of the last expression (4.6) can be realized with complete analogy of the sum (2.7). So, one can see that the mixed (geometry/dynamics) scaling properties of sums (2.5), (4.1) and (4.3) contain new possibilities for modeling of a wide class of different self-similar processes.

5. Mathematical Appendix 1. The general solutions of functional equation (2.16)

The solutions of this functional equation is closely related with well-known solutions of difference equations with constant coefficients

$$Y_k = a_{k-1}Y_{k-1} + a_{k-2}Y_{k-2} + \dots + a_0Y_0. \tag{5.1}$$

The solution of this equation (when all roots are different) can be written as

$$Y_k = K_1 \lambda_1^k + K_2 \lambda_2^k + \dots + K_k \lambda_k^k. \tag{5.2}$$

If one of the roots is degenerate then the solution is (the integer value g defines the degeneracy order)

$$Y_k = \left[\sum_{s=0}^{g-1} (C_s k^s)\right] \lambda_g^k. \tag{5.3}$$

For both cases the desired roots are found from the polynomial

$$P(\lambda) = \lambda^k - a_{k-1}\lambda^{k-1} - a_{k-2}\lambda^{k-2} - \dots - a_0 = 0.$$
 (5.4)

In complete analogy with these well-known solutions one can write the general solution of the functional equation (2.16) for nondegenerate case (making the formal replacement $K_s \to PR_s(z), k \to z/T$)

$$S(z) = \sum_{1}^{k} PR_s(z) \lambda_s^{\frac{z}{T}} = \sum_{s=1}^{k} PR_s(z) \exp^{\frac{\ln(\lambda_s)}{T}z}$$
 (5.5)

and for the case, when one of the roots is g-fold degenerated,

$$S(z) = \left[\sum_{s=0}^{g-1} PR_s(z) z^s \right] \lambda_g^{\frac{z}{T}}.$$
 (5.6)

In expressions (5.5) and (5.6) the constants K_s are replaced by periodic functions $PR_r(z \pm T) = PR_r(z)$, which can be presented by the following decomposition to the Fourier series

$$PR_r(z) = A_0^r + \left[\sum_{k=1}^{\infty} Ac_k^{(r)} \cos(\pi k \frac{z}{T}) + As_k^{(r)} \sin(\pi k \frac{z}{T}) \right], \ r = 1, 2 \cdots, k(5.7)$$

The general solution for the functional equation (2.15) can be obtained from expressions (5.5), (5.6) and (5.7) with the help of formal replacement $z \to ln(z), T \to \xi, \ \nu_r = \frac{ln(\lambda_r)}{ln(\xi)}$.

6. Mathematical Appendix 2

The evaluation of the sum in expression (4.6), namely

$$R_{N(z)} = \frac{c_0}{\tilde{b}^{ln(2)}} \sum_{j=N+1}^{2N} \tilde{b}^{ln(j)} f(z\tilde{\xi}^{ln(j)}), \tag{6.1}$$

is presented below.

For evaluation of the sum (6.1) one can use the following estimation:

$$R_{N}(z) = \frac{c_{0}}{\tilde{b}^{ln(2)}} \left(\tilde{b}^{ln(N+1)} f(z\tilde{\xi}^{ln(N+1)}) + \cdots + \tilde{b}^{ln(N+k)} f(z\tilde{\xi}^{ln(N+k)}) + \cdots + \tilde{b}^{ln(2N)} f(z\tilde{\xi}^{2N}) \right)$$

$$\cong \frac{c_{0}}{\tilde{b}^{ln(2)}} \left(\tilde{b}^{ln(N)} f(z\tilde{\xi}^{ln(2N)}) \sum_{k=1}^{N} \tilde{b}^{\frac{k}{N}} \right)$$

$$N \gg 1 \atop \cong \left(\tilde{b}^{ln(N)} \frac{1 - \tilde{b}}{1 - \tilde{b}^{-1/N}} f(z\tilde{\xi}^{ln(2N)})\right). \tag{6.2}$$

In the last expression we used the following approximation

$$\frac{ln(N+k)}{ln(N)} \cong 1 + \frac{k}{Nln(N)} + \cdots \tag{6.3}$$

and replaced approximately the function

$$f(z\xi^{\ln(N+k)}) \cong f(z\xi^{z\xi^{\ln(2N)}}) \tag{6.4}$$

for all $k \in [1, N]$ by its maximal value.

Acknowledgements

The first co-author (RRN) wants to say that this work was done in the frame of the scientific research that was accepted by Kazan (Volga region) Federal University for 2012 year "Dielectric spectroscopy and kinetics of complex systems".

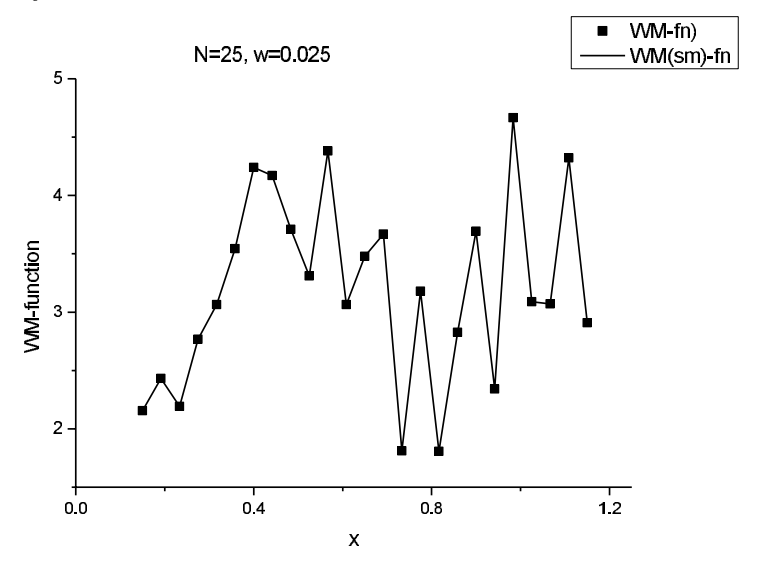


Fig. 1a: The plot of the WM-function for N=25 reference points. The solid line gives the plot of the smoothed WM-function. The value of the smoothing window w=0.025 and so the smoothed WM-function practically coincides with the initial one. Other parameters determining the behavior of this function are given in the text.

See expression (3.3) for details.

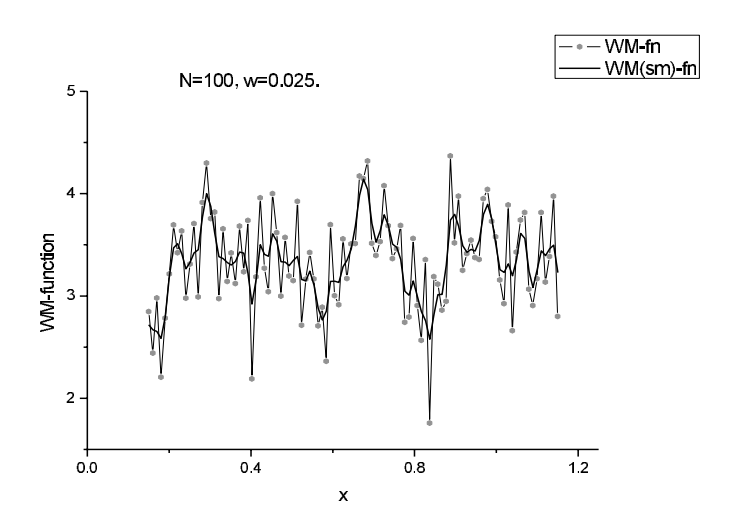


Fig. 1b: The plot of the WM-function for N=100 reference points. The solid line gives the plot of the smoothed WM-function. The value of the smoothing window keeps the same value w=0.025. Other parameters determining the behavior of this function are given by expression (3.3)

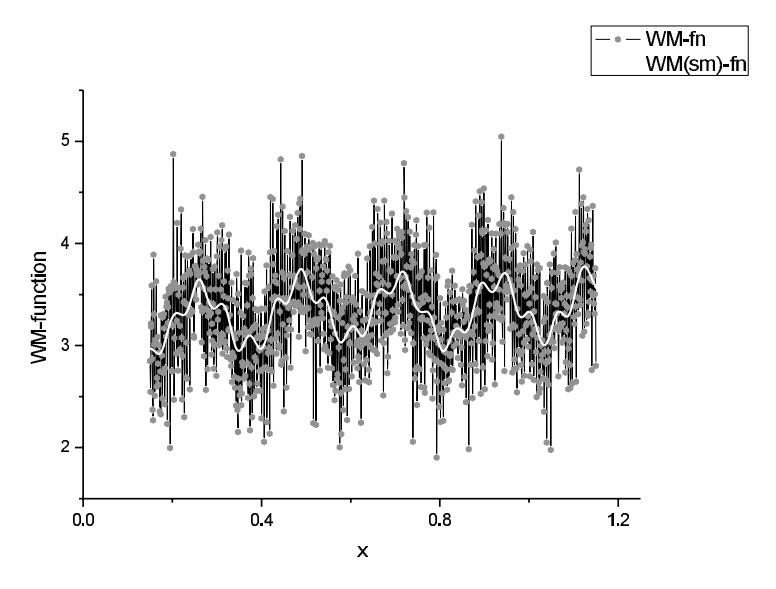


Fig. 1c: The plot of the WM-function for $N{=}1000$ reference points. The white solid line gives the plot of the smoothed WM-function for this case with the same value of the smoothing window w=0.025. Other parameters determining the behavior of this function are given by expression (3.3)

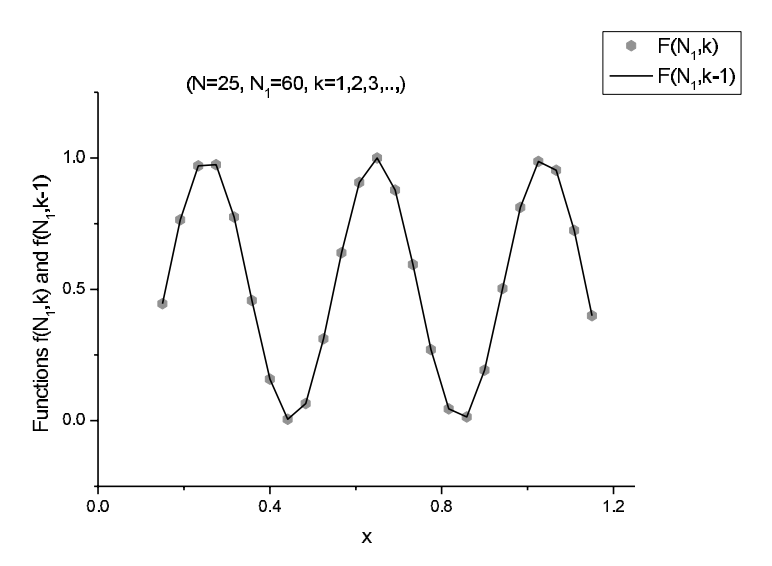


Fig. 2a: The verification of the supposition (2.23) for N=25 points. The verified function is presented by points. The function located on the left-hand side of expression (2.23) is given by solid line. For all tested functions we obtain the following result: the basic contribution comes from the nearest function. The others give the negligible contribution.

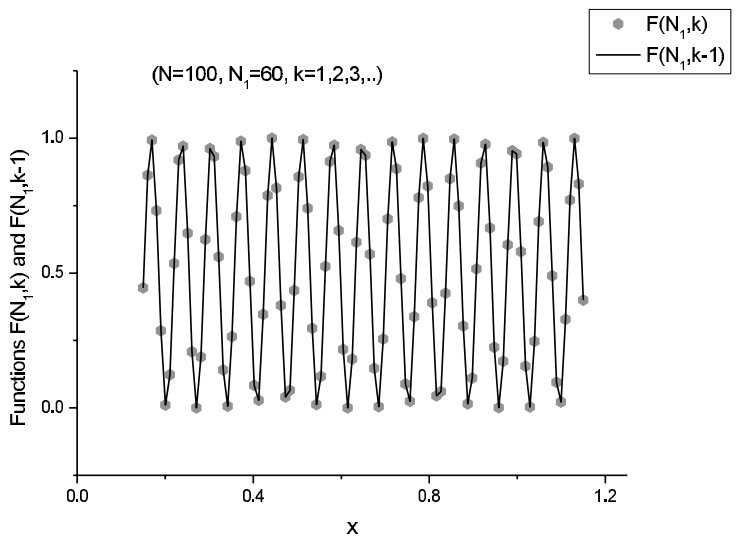


Fig. 2b: The verification of the supposition (2.23) for N=100 points. Again, the verified function is presented by points, the function located on the left of (2.23) is given by solid lines. The test leads to the same conclusion: the basic contribution comes from the nearest function $C_{k-1}=1$. The others give the negligible contribution.

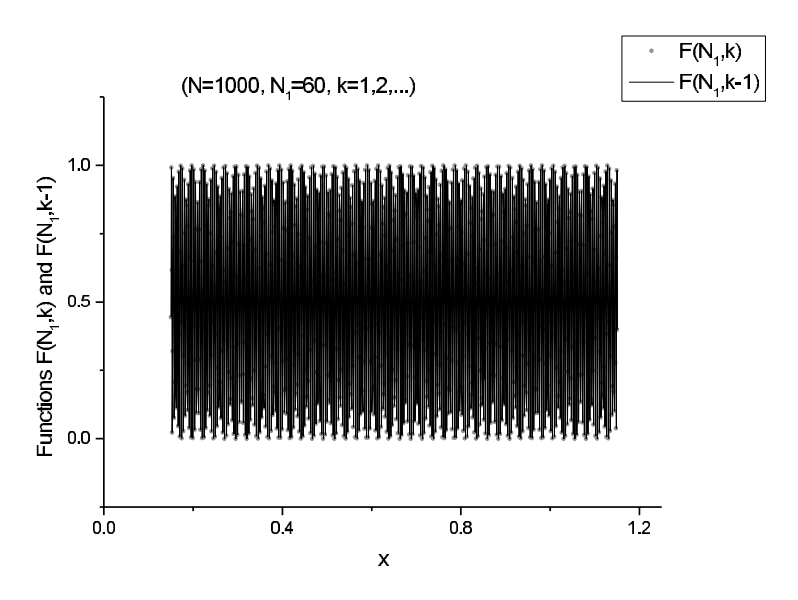


Fig. 2c: The verification of the hypothesis (2.23) for N=1000 points. The test leads to the same conclusion: the basic contribution comes from the nearest function $C_{k-1}=1$.

The contribution of other functions is negligible.

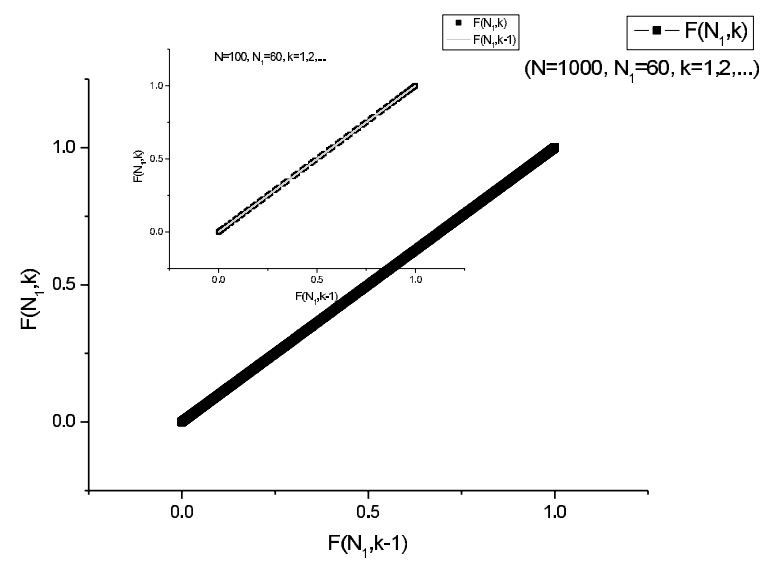


Fig. 2d: The verification of the hypothesis (2.23) for N=100 (small frame above) and 1000 points in another presentation. These functions being plotted with respect to each other give perfect straight lines with the value of the slope equaled one.

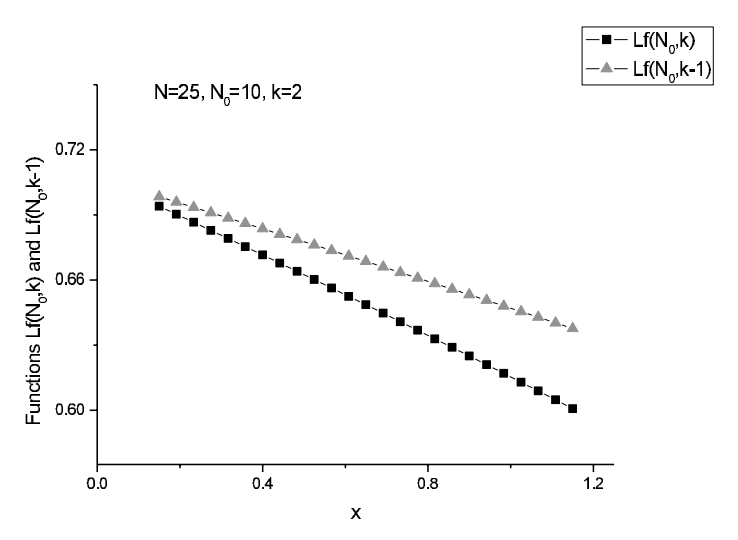


Fig. 3: The low limit verification of the behavior of the function f(x) at x << 1. See expression (2.12). This segment is located in a small interval and so it can be expressed approximately by its mean value as it is expressed by relationship (3.7) The values of this constant lies in the interval [0.01, 0.03] for all range of the reference points considered and so it is not important to give other similar figures for N=100, 1000.

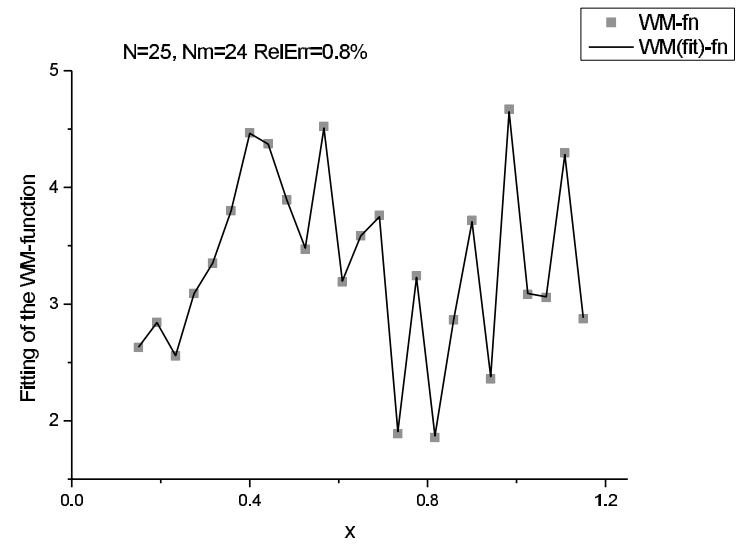


Fig. 4a: This figure demonstrates the result of the WM-function fitting to expression (3.8) For small number of reference points (N=25) the fitting quality is high but in order to provide this high accuracy we took the total number of the fitting constants entering into log-periodic functions (2.20) equaled Nm=24.

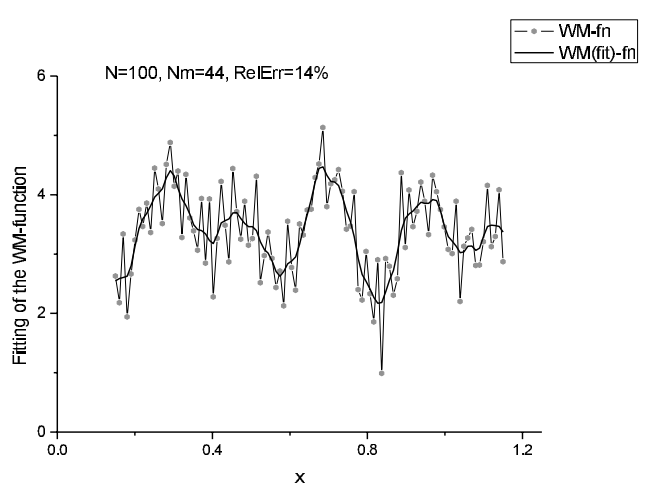


Fig. 4b: This figure demonstrates the result of the WM-function (3.1) fitting to expression (3.8) for N=100. The fitting quality is becoming low and in order to provide accuracy with relative error 14% and provide the visual coincidence with the smoothed function (see Fig.1(b) above) we took the total number of the fitting constants entering into log-periodic functions (2.20) equaled Nm=44.

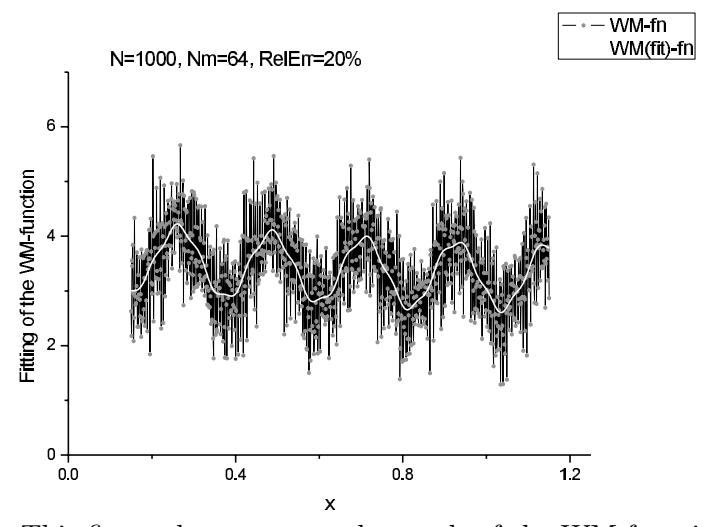


Fig. 4c: This figure demonstrates the result of the WM-function (3.1) fitting to expression (3.8) for N=1000. The fitting quality is becoming worse and in order to provide accuracy with relative error at least 20% and provide the visual coincidence with the smoothed function (see Fig.1 (c) above), we took the total number of the fitting constants entering into log-periodic functions (2. 20) equaled Nm=64.

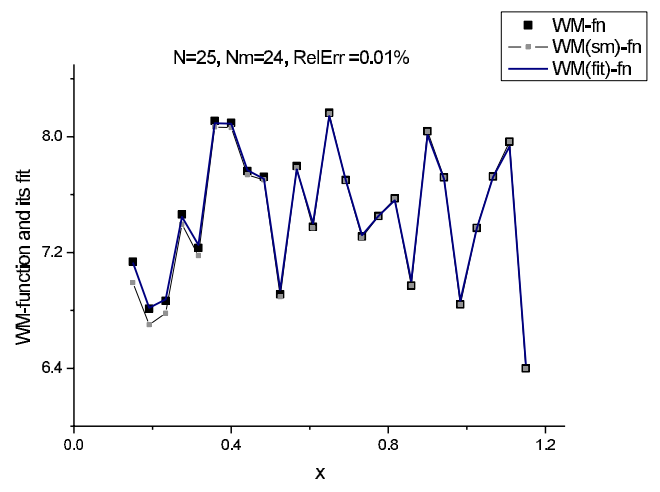


Fig. 5a: This figure shows the behavior of the WM-function for b=1, its smoothed value (shown by grey points) and the fit of this function to expression (3.11) For small number of reference points the quality of the fit is very high (RelErr is equaled to 0.01%). The smoothed function with the same value of the smoothing window (w=0.025) coincides also with this expression. The total number of the fitting constants entering into log-periodic function (2.20) is equaled to Nm=24.

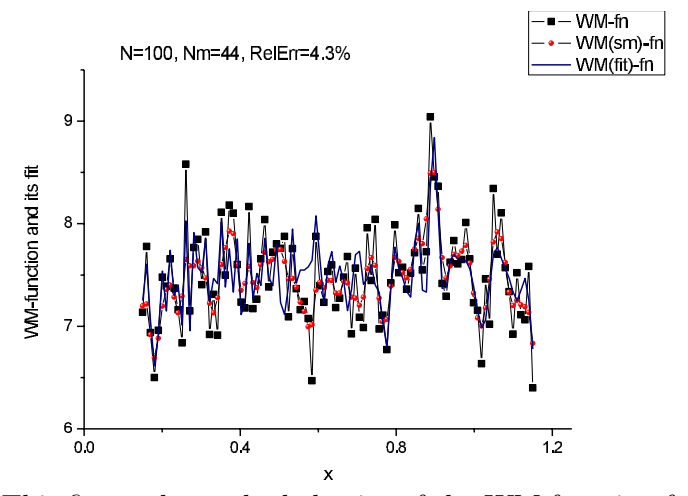


Fig. 5b: This figure shows the behavior of the WM-function for N=100 and b=1, its smoothed value (shown by small red points) and the fit of this function to expression (3.11) is shown by bold navy line. For N=100 the quality of the fit achieves the value RelErr = 4.3%. In order to have a visual coincidence of the fitting function with the smoothed one we used the total number of the fitting constants equaled to Nm=44.

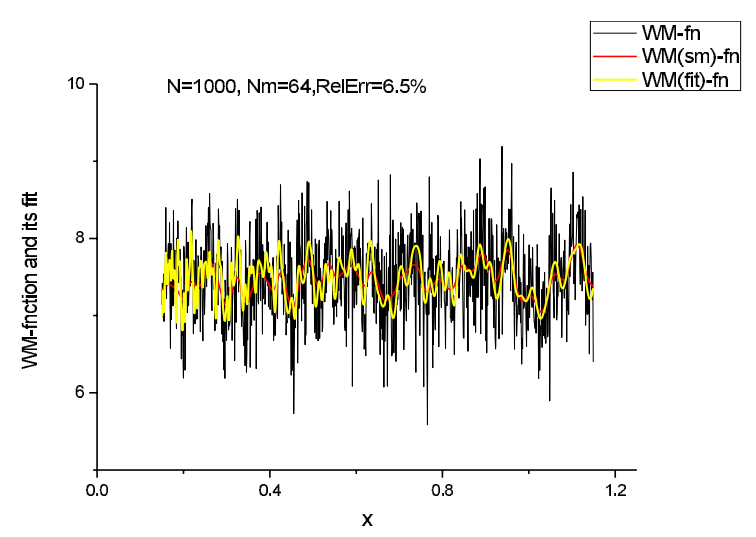


Fig. 5c: This figure shows the behavior of the WM-function for $N{=}1000$ and $b{=}1$. Its smoothed value (shown by bold red line) and the fit of this function to expression (3.11) is shown by bold yellow line. For $N{=}1000$ the quality of the fit is decreased and the value RelErr = 6.5%. Again, in order to have at least a visual coincidence of the fitting function with the smoothed one we used the total number of the

fitting constants from expression (2.20) equaled Nm = 64.

References

- [1] A.A. Arbuzov, R.R. Nigmatullin, Three-dimensional fractal models of electrochemical processes. *Russian J. of Electrochemisty* **45** (2009), 1377–1387.
- [2] D. Baleanu, J.A.T. Machado, A. Luo (Eds.), New Trends in Nanotechnology and Fractional Calculus Applications. Springer (2010).
- [3] G.I. Barenblatt, Scaling, Self-Similarity, and Intermediate Asymptotics. Cambridge University Press (1996).
- [4] E. Capelas de Oliveira, F. Mainardi, J. Vaz Jr., Models based on Mittag-Leffler functions for anomalous relaxation in dielectrics. *Eur. Phys. J. Special Topics* **193** (2011), 161–171.
- [5] J. Feder, Fractals. New York, Plenum Press, p. 283 (1988).
- [6] B. Mandelbrot, *The Fractal Geometry of Nature*. W.H. Freeman, San Francisco (1982).
- [7] A. Le Mehaute, R.R. Nigmatullin, L. Nivanen, Fleches du temps et geometrie fractale. Paris, Editions Hermes (in French) (1998).
- [8] R.R. Nigmatullin, A. Le Mehaute, Is there a geometrical/physical meaning of the fractional integral with complex exponent? *Journal of Non-Crystalline Solids* **351** (2005), 2888–2899.

- [9] R.R. Nigmatullin, Theory of dielectric relaxation in non-Crystalline solids: From a set of micromotions to the averaged collective motion in the mesoscale region. *Physica B: Physics of Condensed Matter* **358** (2005), 201–215.
- [10] R.R. Nigmatullin, Dielectric relaxation based on the fractional kinetics: Theory and its experimental confirmation. *Physica Scripta* T136 (2009), 014001.
- [11] R.R. Nigmatullin, S.O. Nelson, Recognition of the fractional kinetic equations from complex systems: Dielectric properties of fresh fruits and vegetables from 0.01 to 1.8 GH. Signal Proc. 86 (2006), 2744–2759.
- [12] R.R. Nigmatullin, A.A. Arbuzov, F. Salehli, A. Gis, I. Bayrak, H. Catalgil-Giz, The first experimental confirmation of the fractional kinetics containing the complex power-law exponents: Dielectric measurements of polymerization reaction. *Physica B: Physics of Condensed Matter* 388 (2007), 418–434.
- [13] R.R. Nigmatullin, Strongly correlated variables and existence of the universal disctribution function for relative fluctuations. *Physics of Wave Phenomena* **16**, No 2 (2008), 119–145.
- [14] R.R. Nigmatullin, A.P. Alekhin, Calculation of a static potential created by plane fractal cluster. p. 41. In: *Proc. of 3-rd Conference of Nonlinear Science and Complexity* (Ankara, July 28-31, 2010), p. 41.
- [15] J. Sabatier, O.P. Agrawal, J.A. Tenreiro Machado (Eds.), Advances in Fractional Calculus. Springer, (2007).
- [16] D. Sornette, Discrete scale invariance and complex dimensions. *Physics Reports* 297 (1998), 239–270.
- [17] V. Uchaikin, R. Sibatov, Fractional Kinetics in Solids: Anomalous Charge Transport in Semiconductors, Dielectrics and Nanosystems. World Sci. Publ., Singapore (2012).
- ¹ Theoretical Physics Department, Institute of Physics Kazan Federal University, Kremlevskaya str.18, 420008, Kazan, RUSSIA e-mail: renigmat@gmail.com Received: August 8, 2012
- ² Department of Mathematics and Computer Science Cankaya University, 06530, Ankara, TURKEY
- ³ & King Abdulaziz Univ., P.O. Box 80204, Jeddah, 21589 S. ARABIA (on leave from: Inst. of Space Sciences, Magurele-Bucharest, ROMANIA) e-mail: dumitru@cankaya.edu.tr

Please cite to this paper as published in:

Fract. Calc. Appl. Anal., Vol. 15, No 4 (2012), pp. 718–740;

DOI: 10.2478/s13540-012-0049-5